A Dual Band Dual Polarization Slot Patch Antenna for GPS and Wi-Fi Applications

Jianling Chen, Kin-Fai Tong, *Senior Member*, Allann Al-Armaghany, Junhong Wang, *Senior Member*

***Abstract*—In this letter, a dual band and dual polarization capacitive-fed slot patch antenna is investigated. The proposed antenna can operate at 1.575 GHz for Global Positioning System and 2.4 GHz for Wi-Fi system with the corresponding polarizations. A 90° hybrid coupler chip was used to excite the right hand circular polarization required for optimum GPS performance. For the high frequency band, a pair of linearly polarized arc-shaped slots radiating at 2.4 GHz are embedded in the circular patch. The operating bandwidths of the antenna are enhanced by the multi-layered geometry, and the capacitive disks feed points placed between the substrate layers. The measured impedance bandwidths at the lower and high bands are 320 MHz and 230 MHz respectively. The measured 3dB axial ratio bandwidth is 120 MHz.**

***Index Terms*—slot patch antenna, GPS, Wi-Fi, dual-polarization, capacitive feeding.**

I. Introduction

With the rapid development of wireless communication technology, there are continuous demands for devices that can operate at several frequency bands simultaneously. The development of antennas received extensive attention from numerous communication systems [1], [2]. The design challenges of such antennas have been intensified by the further requirements such as retaining low profile, specific polarization at different frequency bands and low fabrication cost [3]–[6]. An example would be at the 1.575 GHz band assigned for Global Positioning System (GPS), a circularly polarized (CP) antenna is essential for optimal performance. In contrast, to support the Wi-Fi wireless communication, a linearly polarized antenna is usually sufficient. A dual-band patch antenna can be a good candidate for both GPS and Wi-Fi antenna design because its ground plane will shield the RF interference from the electronic components, especially in congested enclosures; it can improve the stability and efficiency of the communication links. In various literatures, different techniques were studied to enhance GPS performance [7], [8]. In [9], a compact dual-band circularly polarized GPS antenna, which works at 1.227 GHz and 1.575 GHz has been reported. For multi-band linearly polarization systems, a dual band antenna with arc-shaped slot operating at 1.6 GHz and 2.05-2.29 GHz is reported in [10]. The subtending angle of the slot can be adjusted for operating frequency tuning and band spacing ratio. Furthermore, a triple band H-shaped slot antenna excited by proximity coupling of the microstrip line feed is proposed in [11], it utilized the monopole mode, slot mode, and their higher-order modes to cover the GPS (1.575 GHz) and the two Wi-Fi (2.4-2.485 GHz and 5.15-5.85 GHz) bands. However, the antenna is linearly polarized, and hence its performance at GPS band is compromised. Moreover, A microstrip-fed printed monopole antenna having a parasitic radiator is suggested for GSM, DCS/UMTS/WiBro/2.4 GHz WLAN and 5.2- 5.8 GHz WLAN band applications [12]. This literature study suggests the current antenna designs are capable of operating at multi-bands with only single polarization. These antennas cannot meet the compatible requirements for both GPS and Wi-Fi application. From these instances, it can be seen that designing a multi-band antenna with desired operating frequency, bandwidth and polarization (linear and CP) is a challenging problem.

In this paper, we present a dual-band antenna with appropriate polarizations in the GPS and Wi-Fi bands. The linear polarization performance of the antenna is based on a pair of arc-shaped slots embedded in a circular patch antenna. The patch is fed by two perpendicular capacitive discs in gap-coupled configurations using stacked substrates. The feed points are 90° out of phase that will produce the orthogonal modes for CP at the 1.575 GHz GPS band. The capacitive feeds are loaded by radiating element substrate to enhance the impedance bandwidth for both bands. We demonstrate the detailed geometry, fabrication process and simulation study, which are validated by measurements. The proposed antenna is centered on multi-band communication applications with specific polarization's requirement, while maintaining sufficient gain and high radiation efficiency across all operating bands.

II. Antenna Configuration And Design

The proposed antenna is designed to realize communication devices that require 1.575 GHz (right hand circularly polarized) RHCP GPS and 2.4 GHz Wi-Fi applications. Simulations of the designed three-layer antenna were achieved by using CST Microwave Studio 2013 [13]. Fig. 1(a) shows

Jianling chen and Junhong Wang are with the Department of Electronics and Information Engineering, Beijing Jiaotong University, Beijing, China. (email: 10111002@bjtu.edu.cn,wangjunh@bjtu.edu.cn).

Kin-Fai Tong and Allann Al-Armaghany are with the Department of Electronic and Electrical Engineering, University College London. (email:k.tong@ucl.ac.uk, a.al-armaghany@ucl.ac.uk).

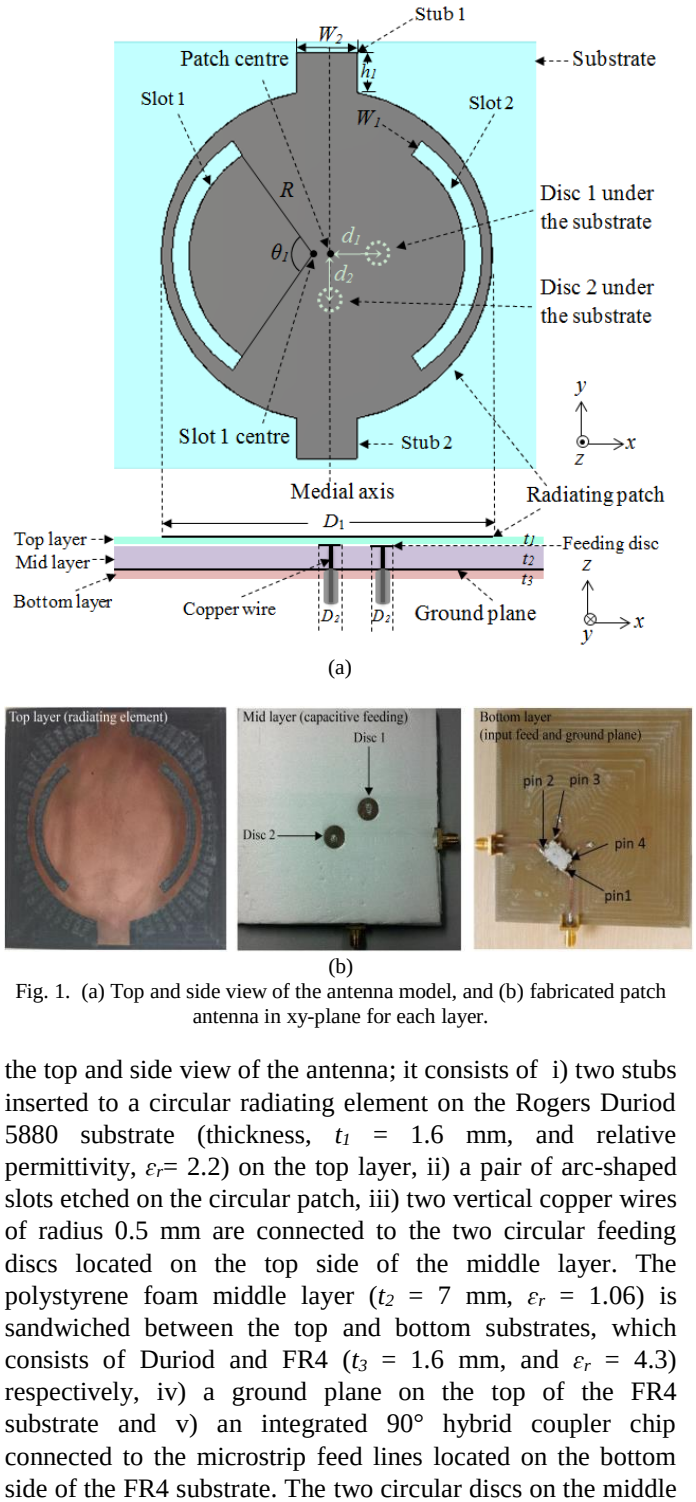

Fig. 1. (a) Top and side view of the antenna model, and (b) fabricated patch antenna in xy-plane for each layer.

the top and side view of the antenna; it consists of i) two stubs inserted to a circular radiating element on the Rogers Duriod 5880 substrate (thickness, t_1 = 1.6 mm, and relative permittivity, ε_r= 2.2) on the top layer, ii) a pair of arc-shaped slots etched on the circular patch, iii) two vertical copper wires of radius 0.5 mm are connected to the two circular feeding discs located on the top side of the middle layer. The polystyrene foam middle layer (t_2 = 7 mm, ε_r = 1.06) is sandwiched between the top and bottom substrates, which consists of Duriod and FR4 (t_3 = 1.6 mm, and ε_r = 4.3) respectively, iv) a ground plane on the top of the FR4 substrate and v) an integrated 90° hybrid coupler chip connected to the microstrip feed lines located on the bottom side of the FR4 substrate. The two circular discs on the middle layer are connected to two outputs of the 90° hybrid coupler through the vertical copper wires. The positions of the feeding discs are optimized for providing the orthogonal mode to achieve CP at 1.575 GHz; therefore, their respective position with the radiating element is essential for optimal performance. The feeding discs are top loaded by the Duriod substrate. The impedance and axial bandwidths are improved by using this feeding approach [15]. The overall dimension of the antenna is 101.6×101.6×10.2 mm^3. The radiating patch is symmetric along the x-axis and y-axis. Two stubs are

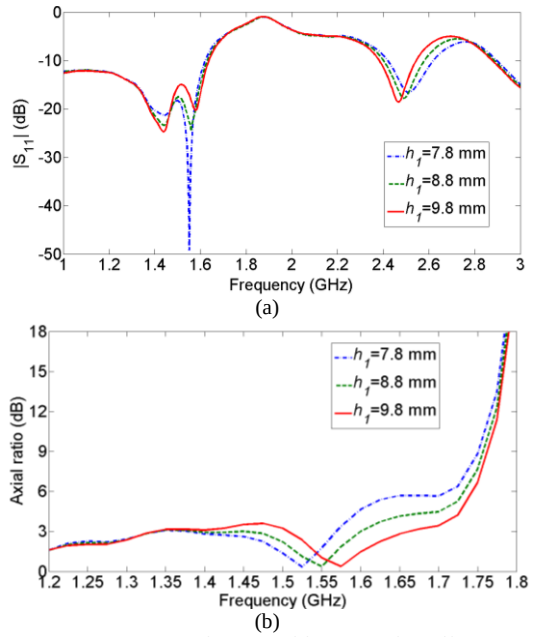

Fig. 2: (a) $|S_{11}|$ and (b) AR as a function of frequency for different heights (h_1) of the stub.

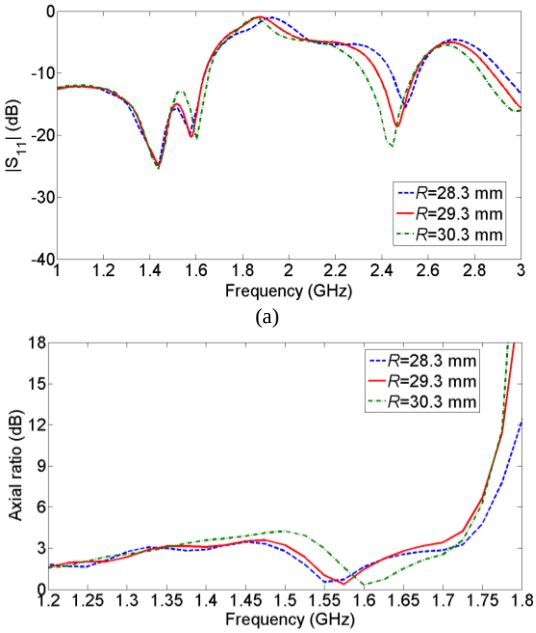

Fig. 3: (a) $|S_{11}|$ and (b) AR as a function of frequency for different radius (R) of the slot.

introduced to the circular patch in the y-plane to increase the electrical length with respect to the horizontal plane (x-plane) to optimize CP operation. An extra resonance at higher frequency, i.e. 2.4 GHz, is induced by adding two symmetrical arc-shaped slots located at the edge of the patch cutting across to the horizontal plane. The other dimensions of the proposed antenna can be found in Table 1.

Fig. 1(b) shows the layers of the fabricated prototype. Pin 1 is connected with the input port, while pin 2 is terminated by a 50Ω load. The output at Pin 3 is 3 dB lower than the input power, and its phase is lagging by approximately 90° to pin 4. Pin 4 is the other output port of the chip with same power of that at Pin 3 [14]. Consequently, Pin 3 and Pin 4 are connected to feed disc 1 and disc 2 respectively to excite the radiating

Diameter of the circular patch, D_1	78.4	Slot inner radius, R	29.3	Height of the stub h_1	9.8
Diameter of the copper feeding discs, D_2	10.0	Width of the slots W_1	4.0	Width of the stub W_2	14
Distance between the centers of the patch to feeding disc 1, d_1	16.0	Distance between the centers of the circular patch and slots d	4.0	Radius of vertical copper wires	5.0
Distance between the centers of the patch to feeding disc 2, d_2	14.0	Subtended angle of the slots, θ_1	114°		

Table 1: Detailed dimensions of the proposed antenna (in millimetres)

element via gap coupling.

From our observation, the height of two stubs, h_1, can be used to optimize the $|S_{11}|$ and axial ratio to desired CP frequency, while the inner radius of the slots, R, will determine the higher band operation frequency of antenna. Therefore, we conducted a parametric study in terms of these two parameters. Fig. 2 shows the $|S_{11}|$ and axial ratio as functions of frequency for different heights (h_1). From the Fig. 2(a), it can be observed that with altered h_1, the weighting of the two orthogonal modes for circular polarization will vary. This is further confirmed by the results showed in Fig. 2(b); the frequency of minimum axial ratio shifts to higher with increasing h_1. In the meantime, the resonant frequency shifts slightly lower with increasing h_1 in the 2.4 GHz band. This may due to the increased equivalent size.

Fig. 3 shows the $|S_{11}|$ and axial ratio as a function of frequency for different slot inner radius, R. From Fig. 3 (a), it can be seen that the 1.575 GHz band is also affected when changing the inner radius of the slots, this is caused by the changing current distribution in the horizontal mode. In contrast, the simulated $|S_{11}|$ bandwidth for 2.45 GHz gets wider and resonant frequency shifts lower with increasing R. This can be explained by the increase in electrical length.

From the Fig. 3 (b), it can be seen that the frequency of the minimum axial ratio shifts to higher with increasing R from 28.3 mm to 30.3 mm.

III. SIMULATION AND MEASUREMENT RESULT

A. $|S_{11}|$ and axial ratio results

Fig. 4 shows the simulated and measured $|S_{11}|$ of the proposed antenna. The performance of the 90° hybrid coupler chip was first measured independently and stored in a s4p file. Then the measured results of the 90° hybrid coupler chip were embedded into the CST simulation. It can be seen that the antenna can operate at both bands of 1.575 GHz and 2.4 GHz. Reasonable agreement between the simulated and measured results was obtained. It can be observed, that the measured $|S_{11}|$ slightly shifted. The deviation is primarily caused by the fabrication process, particularly the stacked foam layers to archive the desired thickness t_2. The measured impedance bandwidth $|S_{11}|$ <-10 dB) is from 1.31 to 1.63 GHz and 2.36 to 2.59 GHz, which is sufficient for both GPS and Wi-Fi operations. Fig. 5 shows the simulated and measured axial ratio of the proposed patch antenna. The measured 3dB axial ratio at 1.575 GHz is about 7.6% from 1.55 to 1.67 GHz. The

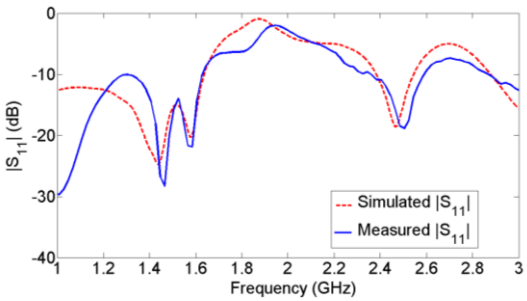

Fig. 4: Simulated and measured $|S_{11}|$.

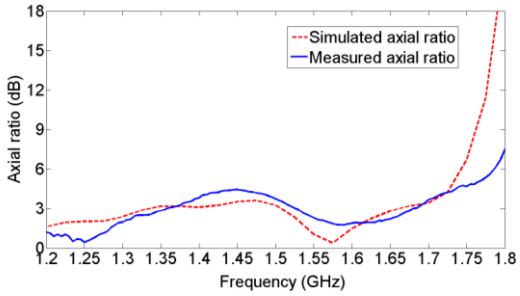

Fig. 5: Simulated and measured axial ratio.

result shifts slightly higher at 1.575 GHz when comparing to the simulated one.

B. Surface distribution at 1.575 GHz and 2.45 GHz

Fig. 6 (a) and (b) show current distributions of the patch at 1.575 GHz and 2.45 GHz respectively. For the case of surface current shown in Fig. 6 (a), the slots and the stubs with the patch provide the orthogonal electrical path horizontally and vertically in xy-plane respectively. For the case of surface current shown in Fig. 6 (b), the slots themselves also provide a shorter electrical path horizontally which produces an upper resonant frequency at 2.45 GHz.

C. Simulated and measured radiation pattern

Radiation patterns are measured at the two resonant frequencies using anechoic chamber. The measured far-field radiation pattern is then compared against the simulation results. Fig. 7 (a) and (b) show the simulated and measured radiation patterns at 1.575 GHz in xz-plane and yz-plane respectively. The measured antenna gain at boresight direction was approximately 6.2 dBi. The 3dB beam width is about 72°, which is 3° wider than simulation. In the LHCP measurement, i.e. cross-polarization, the boresight gain has dropped by about 14.6 dB, as this feeding geometry is not optimal for LHCP.

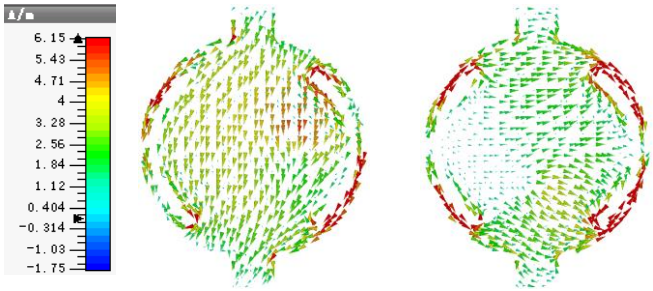

(a)

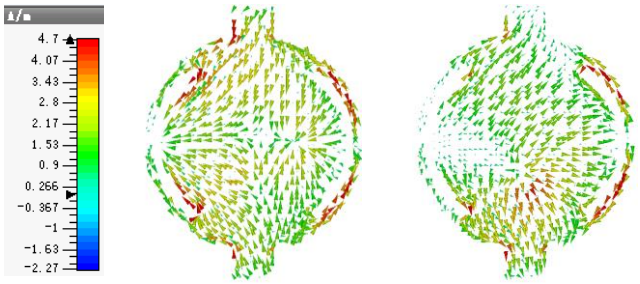

(phase=0°) (phase=90°)

(b)

Fig. 6: Simulated current distribution at (a) 1.575 GHz and (b) 2.45 GHz

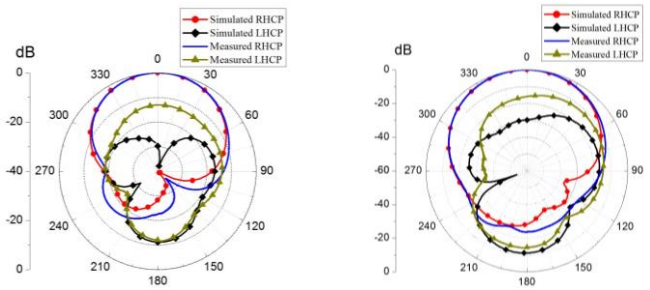

(a) (b)

Fig. 7: Simulated and measured radiation pattern at 1.575 GHz in (a) xz-plane and (b) yz-plane

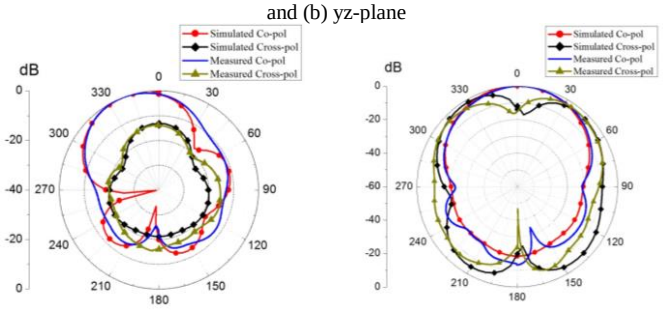

(a) (b)

Fig. 8: Simulated and measured radiation pattern at 2.45 GHz in (a) xz-plane and (b) yz-plane

Fig. 8 (a) and (b) show the simulated and measured radiation patterns at 2.45 GHz in xz-plane and yz-plane respectively, giving the antenna gain of 5.5 dBi at 2.45 GHz. The boresight beam in the xz-plane is shifted by 15°. The angular shift can be explained by the asymmetrical current distribution at 2.45 GHz shown in Fig. 6 (b), the slot on the right has higher current density due to feeding port 1. In the yz-plane, the maximum cross polarization is about -2.8 dB, which is relatively high and is introduced by the orthogonal feeding discs.

IV. CONCLUSIONS

This paper presents a new dual band antenna design using a circular patch with two capacitive feeding disks and arc-shaped slots. The performance and results were assessed and compared with simulation. The two symmetric slots were parameterized to achieve the 2.45 GHz resonant frequency band with a gain of 5.5 dBi. The lower GPS band is right-handed circularly polarized, which will support the GPS reception better when compared to those linearly polarized designs reported in the literature. The CP was achieved by the use of the dual 90° phase shift disc feed method. The result clearly shows the measured axial ratio bandwidth is about 120 MHz at the 1.575 GHz band with a boresight gain of 6.2 dBi. The bandwidth of the proposed antenna was enhanced with use of capacitive feeding and the stacked substrates. The achieved bandwidth is 320 MHz at GPS band, and 230 MHz for the Wi-Fi band. Moreover, the measured results are in reasonable agreement with the embedded simulation which used the measured s4p file of the 90° hybrid coupler chip in conjunction with the 3D EM solver.

ACKNOWLEDGMENT

This work is partially supported by the National Program on Key Basic Research Project under Grant No.2013CB328903, and by the National Natural Science Foundation of China under Grant No.61271048.

REFERENCES

[1] R. Cai, S. Lin, G. Huang, and J. Wang, "Simulation and experimental research on the multi-band slot-loaded printed antenna," in *2010 IEEE 12th International Conference on Communication Technology*, 2010, pp. 500–503.

[2] S.-Y. Suh, W. Stutzman, W. Davis, A. Waltho, K. Skeba, and J. Schiffer, "A novel low-profile, dual-polarization, multi-band base-station antenna element - the fourpoint antenna," in *IEEE 60th Vehicular Technology Conference*, 2004. VTC2004-Fall. 2004, 2004, vol. 1, pp. 225–229.

[4] J. K. H. Gamage, M. Engjom, and I. A. Jensen, "Design of a low profile multi-band antenna for vehicular communication system." *in Antennas and Propagation (EuCAP), 2013 7th European Conference* on, 2013, pp. 1273–1277, 2013.

[3] J. Zhu, M. A. Antoniades, and G. V. Eleftheriades, "A Compact Tri-Band Monopole Antenna With Single-Cell Metamaterial Loading," *IEEE Trans. Antennas Propag.*, vol. 58, no. 4, pp. 1031–1038, Apr. 2010.

5] J. Chen, K.-F. Tong, and A. Al-Armaghany, "A GPS/Wi-Fi dual-band arc-shaped slot patch antenna for UAV application," in *2013 Loughborough Antennas & Propagation Conference (LAPC), 2013*, pp. 490–493.

[6] J. Chen, K.-F. Tong, and J. Wang, "A triple band arc-shaped slot patch antenna for UAV GPS/Wi-Fi applications," ," in *Antennas Propagation (ISAP), 2013 Proceedings of the International Symposium* , vol. 01, pp. 367–370, 2013.

[7] M. K. Alsliety and D. N. Aloi, "A Study of Ground-Plane-Level and Vehicle-Level Radiation Patterns of GPS Antenna in Telematics Applications," *Antennas Wirel. Propag. Lett.*, vol. 6, no. 11, pp. 130–133, 2007.

[8] L. I. Basilio, R. L. Chen, J. T. Williams, and D. R. Jackson, "A New Planar Dual-Band GPS Antenna Designed for Reduced Susceptibility to Low-Angle Multipath*," IEEE Trans. Antennas Propag.*, vol. 55, no. 8, pp. 2358–2366, Aug. 2007.

[9] M. Chen and C.-C. Chen, "A Compact Dual-Band GPS Antenna Design," *IEEE Antennas Wirel. Propag. Lett.*, vol. 12, pp. 245–248, 2013.

[10] G.-B. Hsieh and K.-L. Wong, "Inset-microstrip-line-fed dual-frequency circular microstrip antenna and its application to a two-element dual-frequency microstrip array*," IEE Proc. - Microwaves, Antennas Propag.*, vol. 146, no. 5, p. 359, 1999.

[11] T.-H. Chang and J.-F. Kiang, "Compact Multi-Band H-Shaped Slot Antenna," *IEEE Trans. Antennas Propag.*, vol. 61, no. 8, pp. 4345–4349, Aug. 2013.

[12] K. Seol, J. Jung, and J. Choi, "Multi-band monopole antenna with inverted U-shaped parasitic plane," *Electronics Letters*, vol. 42, no. 15. p. 844, 2006.

[13] CST Microwave Studio 2013 - user manual. .

[14] "Model X3C17A1-03WS Model X3C17A1- datasheet."

[15] Vandenbosch, G.A.E., and Van de Capelle, A.R.: 'Study of the capacitively fed microstrip antenna elements', *IEEE Trans. Antennas Propag.*, 1994, 42, (12), pp. 1648–1652